Journal of Chromatography A, 1419 (2015) 26–36

Contents lists available at ScienceDirect

Journal of Chromatography A

journal homepage: www.elsevier.com/locate/chroma

Isolation, characterisation and quantification of the main oligomeric macrocyclic ellagitannins in *Epilobium angustifolium* by ultra-high performance chromatography with diode array detection and electrospray tandem mass spectrometry

Nicolas Baert*, Maarit Karonen, Juha-Pekka Salminen

Laboratory of Organic Chemistry and Chemical Biology, Department of Chemistry, University of Turku, Turku FI-20014, Finland

ARTICLE INFO

Article history:
Received 18 June 2015
Received in revised form 1 September 2015
Accepted 16 September 2015
Available online 21 September 2015

Keywords:
Willowherb
Oligomeric ellagitannin
Plant phenolic fingerprint
Multiple Reaction Monitoring

ABSTRACT

Tannins have beneficial effects in animal nutrition as they are able to decrease methane emission in ruminants and exert anthelminthic activity against intestinal nematodes. However, tannins can have very diverse structures and therefore, different activities. In order to enhance the research in tannin-rich forages we need tools which are able to quantify tannins individually. In this study we isolated and characterised the main tellimagrandin I (TI)-based oligomeric ellagitannins (ETs) from *Epilobium angustifolium* (willowherb) and developed a UHPLC-DAD–ESI-MS/MS method to quantify them in plant extracts. The mass spectrometer was operated in Multiple Reaction Monitoring mode to enable the selective detection of dimeric to heptameric ETs from the plant extract. The method proved to be sensitive, with limits of detection ranging from 0.1 to 1.3 $\mu g\,mL^{-1}$. The stability test showed a good repeatability with an inter-run deviation of the results from 0.1 to 5%, except for the pentamer and hexamer where it reached 8%. The method was then successfully applied to evaluate the distribution of those ETs in the plant. This work also provides the first time evidence of the presence of tetrameric to heptameric TI in willowherb.

1. Introduction

Tannins are polyphenolic plant secondary metabolites that have demonstrated the ability to reduce methane emission in ruminants [1–3] and to possess anthelminthic activity against intestinal nematode infections [4,5]. However, tannins are a vast family of molecules that shows an incredibly diverse array of chemical structures across the plant kingdom. They are subject to quantitative, seasonal [6,7] and inter-species [8,9] variations and are not evenly distributed—in both quality and quantity—across the different organs of a plant [10]. Several studies also demonstrate that distinct tannin structures can have different chemical and biological activities or at least different levels of those activities (e.g. protein precipitation capacity, anti-/pro-oxidant activity) [11,12]. Furthermore, the activity of polyphenols may vary depending upon their concentration. It has been shown that tannic acid, ellagic acid, gallic acid and flavonoids act as an antioxidant at low concentration but tend to become more pro-oxidant as their concentration increases, or in the presence of Cu(II) [13–15]. All together, these findings highlight the relevance of both identification and quantification of tannins in plants when trying to understand how tannin-rich forages interact with animals' organisms.

To date, the most commonly used methods for the quantification of tannins in plant matrices consist in the acidic hydrolysis of tannins and the subsequent quantification of the hydrolysis products [16,17]. Such methods can estimate the total quantity of each major class of tannins: condensed tannins, gallotannins and ellagitannins (ETs) but completely disregard the structural heterogeneity of the compounds within each class. Analytical methods using HPLC and UV-detection allow compound-specific quantification provided a good chromatographic separation of the analytes [18–20]. However, tannins tend to produce large, multiple peaks or humps in HPLC and UV-detection is not always a satisfactory way to ascertain the purity of a peak. In addition, true concentrations of specific tannins are difficult to obtain as pure native standards are not commercially available. This is especially true for the large ET oligomers that are more complex to separate and purify than their monomeric constituents. This fact is highlighted in the current study that reports the first time purification of even ET hexamers and heptamers while the purification barrier was earlier at the pentamer range.

* Corresponding author. Tel.: +358 2 333 6755.
E-mail address: nicolas.baert@utu.fi (N. Baert).

http://dx.doi.org/10.1016/j.chroma.2015.09.050
0021-9673/

Ultra-high performance liquid chromatography coupled with tandem mass spectrometry (UHPLC–MS/MS) offers a highly selective method that remains compatible with quantitative purposes [21,22]. On one hand, UHPLC combines a good separation of the analytes with a high throughput and low solvent consumption; on the other hand, triple quadrupole-mass spectrometry (QqQ-MS) enables the Multiple Reaction Monitoring (MRM), a technique that can selectively detect and quantify several targeted ions within a single run. UHPLC–MS/MS is thus a powerful tool for the analysis of plant secondary metabolites because it enables the detection and the quantification of individual compounds [23,24]. Moreover, with such method, plant extracts do not require any additional processing, contrary to the hydrolytic methods.

Willowherb (*Epilobium angustifolium*) has been extensively studied and its extracts have shown photoprotective, anti-inflammatory, antitumoral, antioxidant and antimicrobial activity in vitro [25–27]. Those activities are often attributed to oenothein B, the most prevalent secondary metabolite in willowherb [28–31]. Oenothein B is a dimeric, macrocyclic ET and the smallest member of a group of TI-based oligomers (heptameric TI is shown as an example in Fig. 1). To date, the largest oligomeric ET reported in the *Epilobium* genus is oenothein A (trimer) [28]. In the present study we report for the first time the presence of dimeric to heptameric TI in willowherb and provide a protocol for their chromatographic separation and purification. The isolated oligomeric ETs were then thoroughly characterised by MS/MS. Finally, a novel, sensitive and specific MRM-based method was developed and successfully applied to the quantification of dimeric to heptameric TI in three different willowherb tissues. It is also worth emphasising that several oligomeric ellagitannins (up to pentamer) from various plant species have been previously isolated and were found to possess interesting biological activities [32–34]. However, there is, to the best of our knowledge, no published method that can quantify oligomeric ETs larger than trimer in any plant sample. Our interest in these molecules is dual as they represent a technical challenge due their large molecular weight on one hand, and may exert potential benefits in animal nutrition on the other hand. Ancient Finnish records indicate that cows fed with willowherb had their milk production increased [35]. Although that weed is not used as fodder any longer, recent studies show that ETs and ET-rich forages have anthelminthic [36] and anti-methanogenic properties [37,38], thus renewing the interest in this old feed.

2. Materials and methods

2.1. Solvents and chemicals

Technical grade acetone from VWR (Haasrode, Belgium) was used for the extractions. Sephadex fractionation was carried out with analR NORMAPUR acetone and methanol from VWR (Fontenay-sous-Bois, France). HiPerSolv CHROMANORM acetonitrile and methanol from VWR (Fontenay-sous-Bois, France) were used for preparative and semi-preparative HPLC. LC–MS CHROMASOLV acetonitrile was used in UHPLC–ESI-QqQ MS and ESI-qTOF MS analyses (Sigma–Aldrich, Steinheim, Germany). Water was purified with a Millipore Synergy water purification system from Merck KGaA (Darmstadt, Germany). Formic acid 98–100% was from Sigma–Aldrich (Seelze, Germany). Sephadex LH-20 was purchased from GE Healthcare (Uppsala, Sweden). RP-18 LiChroprep 40–63 μm (Darmstadt, Germany) was used as the stationary phase in preparative HPLC.

2.2. Isolation and purification of the oligomeric ellagitannins

2.2.1. Extraction

Fresh willowherb flowers (2 kg) were macerated in 10 L of acetone for 48 h at 4 °C. The liquid phase was removed and replaced by an equal volume of acetone/water (4:1, v/v). Extraction went on for 8 weeks at 4 °C. The extract was then filtered on a filter paper, the acetone was evaporated under reduced pressure and the remaining aqueous solution was frozen and lyophilised, yielding several hundred grams of extract.

2.2.2. First fractionation

Flower extract (30 g) was mixed to a slurry of Sephadex LH-20 (in 100% water). The slurry was then eluted successively with: 3 × 250 mL of water (fraction 1), 3 × 250 mL of methanol/water (1:1, v/v) (fraction 2), 3 × 250 mL of methanol (fraction 3), 6 × 250 mL of acetone/water (4:1, v/v) (fraction 4). Elution was performed in a Büchner funnel (Ø = 240 mm) with a filter paper and using reduced pressure to accelerate the elution. An aliquot of each fraction was analysed by UHPLC-DAD–ESI-MS/MS and the results (not shown) showed that fraction 4 had the highest content in ETs, therefore it was used for the following purification steps. Acetone was evaporated under reduced pressure and the remaining aqueous phase was frozen and lyophilised. This first fractionation step was repeated several times until it yielded a sufficient amount of material for the next steps.

2.2.3. Column chromatography

A slurry of Sephadex LH-20 was loaded into a glass column (40 cm × 4.8 cm i.d., Kimble-Chase Kontes™ Chromaflex™) and equilibrated with 1500 mL of ultrapure water at a flow rate of 5 mL min^{-1}. The sample (3 g of fraction 4) was dissolved in 15 mL of ultrapure water, filtered (0.2 μm, PTFE) and applied on top of the gel. Elution was carried out according to the protocol described in supplementary information. An aliquot of each fraction was analysed by UHPLC-DAD–ESI-MS/MS and fractions with a similar composition were combined together. Acetone was evaporated under reduced pressure and the aqueous phase was frozen and lyophilised. This purification step was repeated several times in order to maximise the amount of each fraction. Those Sephadex fractions were further purified by preparative HPLC.

2.2.4. Preparative HPLC

The HPLC unit was constituted of a Waters 2535 Quaternary Gradient module coupled with a Waters 2998 Photodiode Array Detector. Collection was operated automatically by a Waters Fraction Collector III. We used a binary solvent system methanol/0.1% aqueous formic acid at a constant flow rate of 8 mL min^{-1}. The column (30 cm × 2.5 cm i.d.) was packed with RP-18 (40–63 μm). Different elution protocols were used depending on the composition of the fractions. Those protocols are described in supplementary information. The collected fractions were evaporated to dryness overnight using a Savant SC 210A SpeedVac Concentrator coupled with a Savant RVT 5105 Refrigerated Vapor Trap from Thermo Scientific. Individual oligomeric ETs were lastly purified by semi-preparative HPLC.

2.2.5. Semi-preparative HPLC

The HPLC unit was the same as described above. The solvent system was acetonitrile/0.1% aqueous formic acid and was set at 16 mL min^{-1}. The column was a Gemini® 10 μm C18 110 Å AXIA™ packed (150 mm × 212.0 mm internal diameter) from Phenomenex. Different elution protocols were used depending on the composition of the fractions. Those protocols are described in supplementary information. The collected fractions were

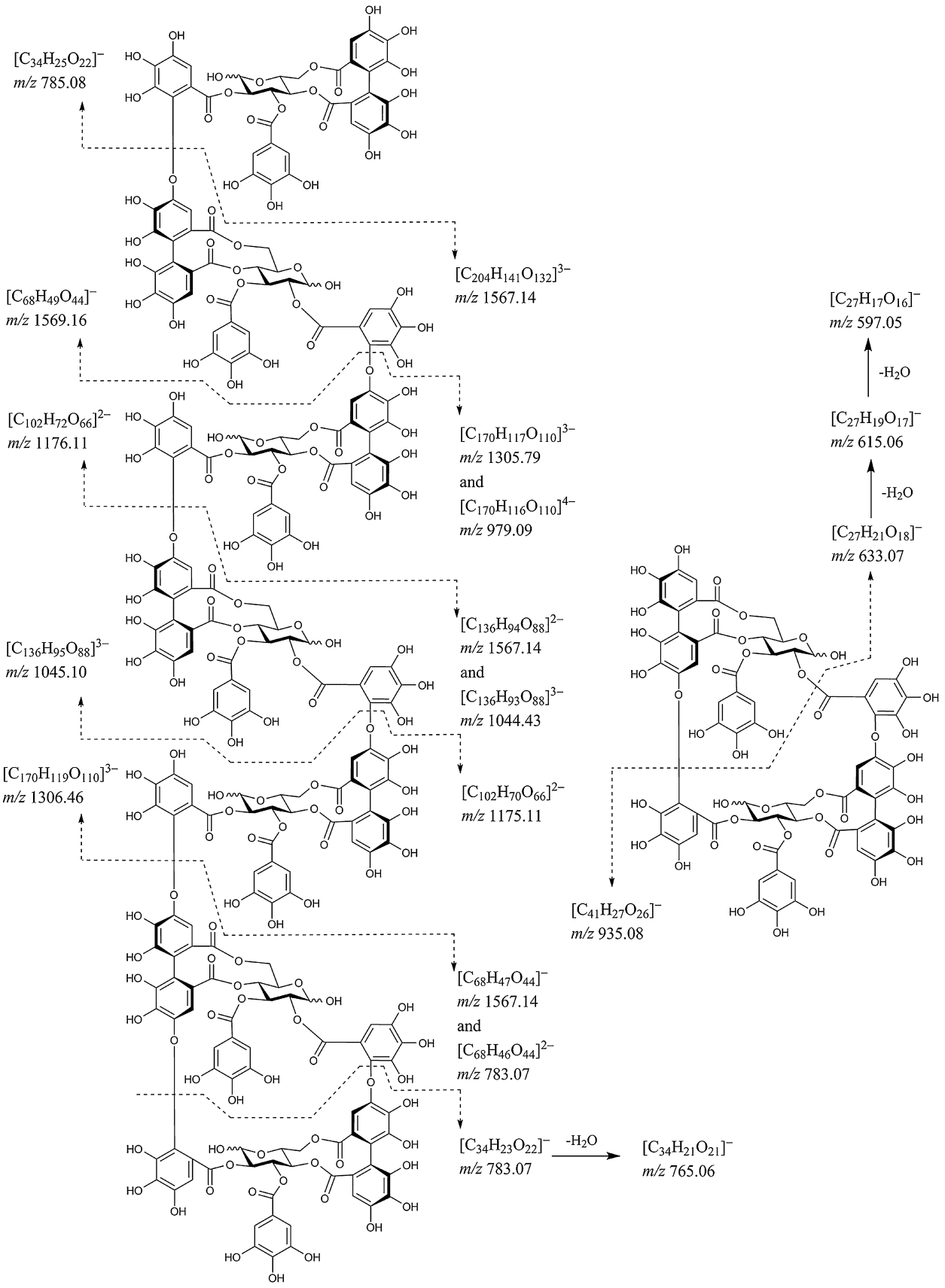

Fig. 1. Fragmentation of heptameric tellimagradin I (left-hand side) illustrates the structure and charge state of the main fragment ions produced in ESI-Qq-TOF-MS/MS by dimeric to heptameric tellimagrandin I. Fragmentation of oenothein B (right-hand side) shows a tentative mechanism for the formation of the ions at *m/z* 935.08 and 633.07 observed with all the 6 oligomeric ellagitannins.

evaporated to dryness overnight using a Savant SC 210A SpeedVac Concentrator coupled with a Savant RVT 5105 Refrigerated Vapor Trap from Thermo Scientific.

2.3. Willowherb test samples

2.3.1. Sample collection

From a single population, 10 flowering *E. angustifolium* (L.) individual plants were harvested in the area of Turku (southwest Finland) in July 2012. Shortly after collection, leaves, stems and flowers from each individual plant were cut off and lyophilised. Once dry, each one of these plant parts was ground into a fine, homogeneous powder with a ball-mill. As a result, we obtained 30 samples (3 plant parts × 10 individuals).

2.3.2. Sample preparation

Extraction was performed on 10 mg of each sample by adding 1400 μL of an acetone/water solution (4:1, v/v). Samples were then shaken for 3 h on a planar shaker in a cold room (4 °C). After centrifugation at 13,500 × *g* for 10 min the supernatant was recovered and stored in a tube and the residue was extracted a second time according to the same protocol. The two acetone/water extracts were combined and concentrated under reduced pressure (20 °C) until complete evaporation of the acetone. The concentrated aqueous extract was frozen and lyophilised.

The lyophilised extract was dissolved in 500 μL of ultra-pure water and vortexed for 10 min. The resulting solution was then filtered by using VWR® 0.2 μm PTFE syringe filters before analysis by UHPLC-DAD–ESI-MS/MS. In parallel, a fraction of the filtered solution was used to produce a 1:31 dilution which was also analysed.

2.4. Analytical methods

2.4.1. UHPLC-DAD–ESI-MS/MS

The UHPLC-DAD–ESI-MS/MS instrument used for all the sample analyses in the present study was an Acquity™ UPLC (Waters Corp., Milford, MA, USA) coupled with a XEVO™ TQ triple-quadrupole mass spectrometer (Waters Corp., Milford, MA, USA). The column was an Acquity UPLC BEH Phenyl 1.7 μm, 2.1 mm × 100 mm (Waters Corp., Wexford, Ireland). Elution was carried out with a binary solvent system consisting of acetonitrile (A) and 0.1% aqueous formic acid (B) at a constant flow rate of 0.5 μL min^{-1}. The elution pattern went as follows: 0–0.5 min: 0.1% A; 0.5–5.0 min: 0.1–30% A (linear gradient); 5.0–5.1 min: 30–90% A (linear gradient); 5.1–7.1 min: 90% A (washing); 7.1–7.2 min: 90–0.1% A (linear gradient); 7.2–8.5 min: 0.1% A (stabilisation). UV–vis (190–500 nm) and MS data (*m*/*z* 100 to 2000) were recorded from 0 to 6 min. The electrospray was set on negative mode and the settings were: capillary voltage: 3.4 kV; desolvation temperature: 650 °C; source temperature: 150 °C; desolvation gas and cone gas (N_2) flow rate: 1000 and 100 L h^{-1}, respectively; collision gas: argon.

2.4.2. ESI-Qq-TOF

To elucidate the structure of the compounds we analysed the purified ETs with an ESI-micrOTOF-Q mass spectrometer (Bruker Daltonics, Bremen, Germany). About 3 mg of each ET (dimer to heptamer) was dissolved in 500 μL of an acetonitrile/H_2O mixture (1:4, v/v), filtered (0.2 μm, PTFE) and analysed via direct infusion. The mass spectrometer was controlled by Compass micrOTOF control software (Bruker Daltonics) and operated in negative mode. The capillary voltage was maintained at +4000 V with the end plate offset at −500 V. The nebuliser gas (N_2) pressure was set at 0.4 bar, the flow rate of the drying gas (N_2) was 4.0 L min^{-1} and its temperature was set at 200 °C. Masses were scanned from *m*/*z* 100 to 2000. The calibration of the instrument was performed with a 5 mM sodium formate solution injected by direct infusion before the sample analyses in order to provide high-accuracy mass measurements. Data were processed by Compass DataAnalysis software (version 4.0, Bruker Daltonics). For each ET we selected the major molecular ion and performed MS/MS fragmentation of it by gradually increasing the collision energy in the collision chamber (argon was used as collision gas). A software-assisted (Bruker Daltonics DataAnalysis 4.0) calculation of the chemical formula was also performed using the monoisotopic peak of the molecular ion.

2.5. Standards

2.5.1. Ionisation reference

A solution of pure oenothein B (2.40 μg mL^{-1}) was analysed 5 times every 2 h in order to monitor the ionisation efficiency within a run or between runs and to correct the measured peak areas accordingly.

2.5.2. Standard purity

The purity of the isolated oligomeric ETs as evaluated by UHPLC-DAD–ESI-MS/MS was: oenothein B (99.9%), oenothein A (99.4%), tetramer (98.7%), pentamer (72.9%), hexamer (97.7%), heptamer (95.5%).

2.5.3. Calibration curves

The quantification method shown in the present study was based on the utilisation of external calibration curves. For each one of the six oligomeric ETs, a serial dilution (in acetonitrile/H_2O, 1:4, v/v) was produced using the following concentrations: oenothein B (0.06, 0.3, 1.5, 6, 15, 30, 60, 90 μg mL^{-1}), oenothein A and tetramer (0.3, 1.5, 6, 15, 30, 60, 90, 150 μg mL^{-1}), pentamer (0.9, 3.5, 8.8, 17.5, 35, 53, 88 μg mL^{-1}), hexamer (0.24, 1.2, 4.8, 12, 24, 48, 72, 120 μg mL^{-1}) and heptamer (0.3, 1.5, 6, 15, 30, 60, 90, 150 μg mL^{-1}). Calibration curves were analysed in triplicate by UHPLC-DAD–ESI-MS/MS using the MRM transitions developed in 2.2.6. Average peak area versus concentration was plotted. Origin 8.0 software was used to calculate linear and polynomial regression equations as well as regression coefficients. Weighted fitting method was used, with weighting set as $1/\omega^2$ (where ω is the standard error).

2.6. Method validation

2.6.1. Limit of detection and limit of quantification

The limits of detection and quantification for each compound were calculated using the calibration plot method [39]. The formulas were: $LOD = 3\sigma_b/a$ and $LOQ = 3 \times LOD$, where a and b are the slope and y-intercept of the linear regression, respectively, and σ_b is the estimated standard deviation of the y-intercept.

2.6.2. Repeatability

To assess the repeatability of the method, 10 replicates of flower, leaf and stems samples (each one in non-diluted and 32-times diluted forms) were analysed 3 days in a row. The stability of the results for the measurement of dimeric to heptameric ETs was calculated and expressed as the relative standard deviation of the peak area (RSD) within each run (intra-run RSD) and between runs (inter-run RSD).

2.6.3. Extraction efficiency

Leaf, flower and stem samples of willowherb were submitted to 3 successive extraction steps (according to the method described in Section 2.3.2) in order to assess the efficiency of the extraction protocol. Successive extracts were analysed separately by UHPLC-DAD–MS/MS and oligomeric ETs were quantified.

Table 1
Fragmentation of the tellimagrandin I-based oligomeric ellagitannins from willowherb by ESI-Qq-TOF-MS/MS.

Oligomer size	Pseudo-molecular ion (*m*/*z*)	Fragment ions (*m*/*z*)	Chemical formula	Exact mass (Da)		Error (ppm)
				Measured	Calculated	
Dimer	783.07 $[M-2H]^{2-}$	935.08; 765.06; 698.06[a]; 633.07; 615.06; 597.05; 301.00; 275.02	$C_{68}H_{48}O_{44}$	1568.1522	1568.1518	0.3
Trimer	1175.11 $[M-2H]^{2-}$	1567.14[b]; 1090.10[a]; 935.08; 785.08; 783.07[c]; 765.06; 633.07; 615.06; 597.05; 301.00; 275.02	$C_{102}H_{72}O_{66}$	2352.2132	2352.2278	6.2
Tetramer	1044.43 $[M-3H]^{3-}$	1569.16; 1567.14[b]; 1175.11; 987.75[a]; 935.08; 785.08; 783.07[d]; 765.06; 633.07; 615.06; 597.05; 301.00; 275.02	$C_{136}H_{96}O_{88}$	3136.2876	3136.3037	5.1
Pentamer	1305.79 $[M-3H]^{3-}$	1569.16; 1567.14[e]; 1249.11[a]; 1176.11; 1175.11; 935.08; 785.08; 783.07[c]; 765.06; 633.07; 615.06; 597.05; 301.00; 275.02	$C_{170}H_{120}O_{110}$	3920.3595	3920.3796	5.1
Hexamer	939.88 $[M-5H]^{5-}$	1569.16; 1567.14[b]; 1305.79; 1176.11; 1175.11; 1045.10; 1044.43; 979.09; 935.08; 785.08; 783.07[d]; 765.06; 633.07; 615.06; 597.05; 301.00; 275.02	$C_{204}H_{144}O_{132}$	4704.4285	4704.4555	5.7
Heptamer	1371.13 $[M-4H]^{4-}$	1569.16; 1567.14[f]; 1328.62[a]; 1306.46; 1305.79; 1176.11; 1175.11; 935.08; 785.08; 783.07[d]; 765.06; 633.07; 615.06; 597.05; 301.00; 275.02	$C_{238}H_{168}O_{154}$	5488.4864	5488.5315	8.2

[a] Neutral loss of 170 Da from the molecular ion, which corresponds to a loss of gallic acid.
[b] $[C_{68}H_{47}O_{44}]^-$ only.
[c] $[C_{34}H_{23}O_{22}]^-$ only.
[d] $[C_{68}H_{46}O_{44}]^{2-}$ and $[C_{34}H_{23}O_{22}]^-$.
[e] $[C_{136}H_{94}O_{88}]^{2-}$ and $[C_{68}H_{47}O_{44}]^-$.
[f] $[C_{204}H_{141}O_{132}]^{3-}$ and $[C_{136}H_{94}O_{88}]^{2-}$ and $[C_{68}H_{47}O_{44}]^-$.

2.6.4. Matrix effect

Leaf, flower and stem extracts were prepared as described in Section 2.3.2 (in both diluted and non-diluted version). Diluted extracts were spiked with 20 μL of a solution containing known concentrations of oenothein B, oenothein A, tetramer and pentamer. Non-diluted samples were spiked with 20 μL of a solution containing known concentrations of pentamer, hexamer and heptamer. In parallel, a duplicate of each extract was spiked with 20 μL of a blank solution (acetonitrile/H_2O 1:4, v/v). Samples were analysed by UHPLC-DAD–MS/MS and oligomeric ETs were quantified in all the extracts using the calibration curves presented in Section 2.5.3. The matrix effect was calculated for each oligomeric ET, in all three matrices using the equation described by Caban et al. [40]:

$$\text{Matrix effect}\,(\%) = \left(\frac{\text{Quantity in spiked sample} - \text{Quantity in nonspiked sample}}{\text{Quantity in spiking solution}} - 1 \right) \times 100$$

3. Results and discussion

3.1. Ellagitannins identification by ESI-Qq-TOF MS

Oenothein B and A have been previously reported in *Epilobium* species [41] and their structures have been characterised by NMR [42,43]. Oenothein B is made of two TI monomers linked together by two *m*-DOG-type bonds between the HHDP groups and the galloyl groups in C_2 position on the glucopyranose ring. Oenothein A is constructed by attaching one TI monomer to oenothein B via a single *m*-DOG-type bond between one HHDP moiety of oenothein B and the C_2 galloyl group of TI. The structures of larger oligomers are hypothesised to follow the same pattern: addition of one TI via a single *m*-DOG-type bond. Previous MS/MS analyses of tetrameric to heptameric TI suggest that the elongation of the oligomer always occurs at the same end of the molecule, therefore producing asymmetric oligomers with an oenothein B core at one end, and a chain of singly bound TI units at the other end [44]. Heptameric TI is shown in Fig. 1 to illustrate this pattern. Dimeric to heptameric TI have been previously identified from crude extracts and Sephadex fractions of *Oenothera biennis* (evening primrose) [44,45]. However, in the present study, we show for the first time the MS/MS analyses of pure oligomeric ETs (up to heptamer), and thus a more comprehensive understanding of their fragmentation patterns.

3.1.1. Pseudo-molecular ions

The main pseudo-molecular ion for each oligomeric ET is shown in Table 1 and was selected as the precursor for ESI-qTOF-MS analysis. It is interesting to note that the main pseudo-molecular ions that were observed in ESI-qTOF-MS for hexamer and heptamer were not the same as in ESI-QqQ-MS. For the hexamer, $[M-5H]^{5-}$ (*m*/*z* 939.9) showed a stronger signal in ESI-qTOF-MS than the $[M-3H]^{3-}$ (*m*/*z* 1567.9). For the heptamer, $[M-4H]^{4-}$ (*m*/*z* 1371.1) had higher intensity than the $[M-3H]^{3-}$ (*m*/*z* 1829.3) which was used to create the MRM transitions. Theoretical chemical formulas for each compound were calculated by the software, using the monoisotopic peak of the molecular ion. Results (shown in Table 1) show a good concordance with the formulas that have been previously hypothesised for tetramer to heptamer, thus supporting their putative structures.

3.1.2. Fragmentation pattern

The *m*/*z* values of the main fragments are listed in Table 1. As previously observed by Karonen et al. [44], the DOG-type bonds between monomers were the most easily cleaved. Consequently, the main fragment ions are constituted of either a chain of singly bound TI units or a chain of singly bound TI units terminated with two TI units doubly bound to one another. This fragmentation pattern is illustrated in Fig. 1 with the example of heptameric TI, which conveniently encompasses the main fragments observed with the smaller oligomers.

Additionally to those TI-based fragments, a singly charged ion at *m*/*z* 765.06 was found with all the oligomers and was the most predominant peak when collision energy was in the range of 20–25 eV. A likely hypothesis to explain the formation of that ion is the cleavage of the two DOG-type bonds of the oenothein B unit which would form doubly charged ion of 784 Da. The deprotonated HHDP group subsequently oxidises and forms an *o*-quinone according to a mechanism proposed by Salminen et al. [45]. This oxidation results in a loss of one H^+ and two electrons thus yielding a singly negatively charged fragment of 783 Da that we witnessed with all the oligomers (Fig. 2). That ion then undergoes a neutral loss of 18 Da,

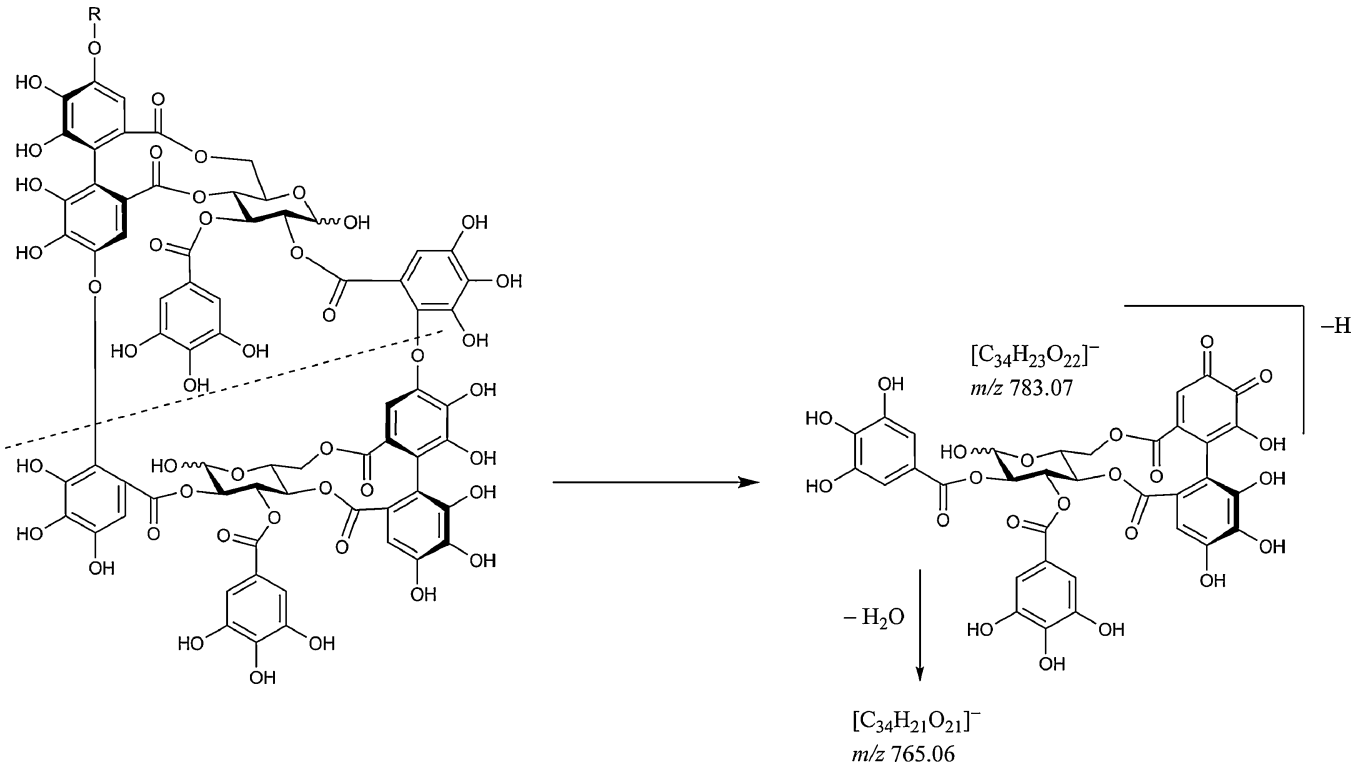

Fig. 2. Putative mechanism for the formation of ions at *m/z* 783.07 and 765.06. The cleavage of the two DOG-type bonds is followed by the oxidation of the HHDP group which forms an *o*-quinone and results in a singly charged ion of 783.07 Da which then undergoes dehydration.

which most likely corresponds to a dehydration process, and forms a singly charged ion at *m/z* 765 (783 – 18 = 765).

The dehydration hypothesis is reinforced by the observation of similar phenomena. Indeed, an ion at *m/z* 633 was witnessed for all the oligomers and was systematically accompanied with ions at *m/z* 615 and 597, all showing relatively similar intensities. The 18 Da difference between those masses suggests sequential water losses (Fig. 1). Such dehydration reactions during fragmentation have been previously observed with gallotannins and galloylglucoses [46]. The 6 oligomers each showed a product ion that corresponded to a neutral loss of 170 Da from their pseudo-molecular ion (Table 2). This type of fragmentation has been reported before and is typical of galloylglucoses. In our case it almost certainly occurs to the gallic acid unit attached to the C_3 position of the glucopyranose ring of one TI monomer. All together these data support the proposed structure of the oligomeric TI and confirm their presence in willowherb.

3.2. MRM optimisation

3.2.1. Development and optimisation of MRM transitions

A 30 μg mL^{-1} solution was prepared for each pure oligomeric ET (in acetonitrile/water, 1:4, v/v) and was injected by direct infusion in ESI-QqQ-MS/MS. The solvent flow in the electrospray was acetonitrile/0.1% aqueous formic acid (1:4, v/v) and was set at a rate of 0.20 μL min^{-1}. Cone voltages were changed from 10 to 60 V with 10 V increments in order to find the voltage that would produce the most efficient ionisation of the molecular ion. The fragments of the main molecular ion were then examined by varying collision energy from 5 to 110 eV by 5 eV increments. A main precursor and a main fragment were thus selected for each oligomer and used to create the MRM transition that was used for quantification (MRM1).

An additional MRM transition was monitored for each oligomeric ET from willwoherb leaf, stem and flower samples in order to ascertain the specificity of the detection. For that secondary transition (MRM2) we kept the same precursor ion as in the main transition but chose the fragment that showed the second highest intensity. The peaks given by those two transitions were integrated separately and their respective areas were used to calculate a ratio = *MRM2*/*MRM1*.

3.2.2. Precursor ions

Because of the *m/z* detection range of the instrument (from *m/z* 40 to 2048) and the molecular mass of the oligomeric ETs, it was only possible to observe multiply charged pseudo-molecular ions. However, a singly charged ion was visible for oenothein B at *m/z* 1567.1 but it systematically showed a lower intensity than the doubly charged ion (*m/z* 783.1) within the tested cone voltage range. For the six oligomers the main pseudo-molecular ion was produced with a cone voltage comprised between 30 and 46 V (Fig. 3). Increasing the voltage further caused in-source fragmentation and the subsequent formation of product ions at *m/z* 301 and 275, which come from the cleavage and rearrangement an HHDP moiety and are thus characteristic of ETs [46].

3.2.3. Fragment ions

The fragment ions were analysed using a wide range of collision energies (from 5 eV to 110 eV). For each oligomer the fragment which showed the highest intensity was retained and utilised for quantification. The product ion with the second highest intensity was used as a means of confirmation. As can be seen in Fig. 3 the fragment ions at *m/z* 301 and 275 were typically formed with rather high collision energies (50 to 90 eV). In most cases, *m/z* 301 was more abundant than *m/z* 275, except for heptamer, where the opposite trend was witnessed. Oenothein B was also an exception as it predominantly produced a fragment at *m/z* 765 with collision energy of 20 eV.

Table 2
Summary of the multiple reaction monitoring parameters.

Compound	Molar mass ($g\,mol^{-1}$)	MRM retention time window (min)	MRM1 quantification (m/z)	CV/CE	MRM2 confirmation (m/z)	CV/CE	MRM2/MRM1 peak area ratio (mean ± SD)
Oenothein B	1569.1	2.80–3.37	$[M-2H]^{2-}$ 783.1 > 765.3	30/20	783.1 > 301.0	30/40	0.87 ± 0.01[a]
Oenothein A	2353.6	3.13–3.58	$[M-2H]^{2-}$ 1175.5 > 301.0	46/52	1175.5 > 275.0	46/62	0.88 ± 0.02[a]
Tetramer	3138.2	3.42–3.95	$[M-3H]^{3-}$ 1044.8 > 301.0	32/50	1044.8 > 275.0	32/60	0.84 ± 0.03[b]
Pentamer	3922.7	3.71–4.20	$[M-3H]^{3-}$ 1306.4 > 301.0	40/65	1306.4 > 275.0	40/75	0.94 ± 0.04[c]
Hexamer	4707.3	3.70–4.70	$[M-3H]^{3-}$ 1567.9 > 301.0	42/90	1567.9 > 275.0	42/70	0.52 ± 0.07[c]
Heptamer	5491.8	3.80–4.80	$[M-3H]^{3-}$ 1829.3 > 275.0	46/75	1829.3 > 301.0	46/100	0.88 ± 0.02[d]

CV, cone voltage (V); CE, collision energy (eV).
[a] Measured on leaves, flowers and stem samples, diluted 32 times ($n = 9$).
[b] Measured on leaves, flowers and stem samples, non-diluted and diluted 32 times ($n = 18$).
[c] Measured on leaves, flowers and stem samples, non-diluted ($n = 9$).
[d] Measured on leaves and flowers samples, non-diluted ($n = 6$).

3.2.4. MRM2/MRM1 ratio

The MRM2/MRM1 ratio showed very little variation overall, with a relative standard deviation <5%, except for the hexamer where it reached 13% (Table 2). More interestingly, that ratio seemed unaffected by the nature of the matrix (leaf, flower or stem) as can be seen from the very low RSD measured for dimer, trimer in diluted extracts and for pentamer and heptamer in non-diluted extracts. Dilution of the extract did not have any significant effect on that ratio either, as can be attested by the low RSD observed with tetramer (measured in all the matrices in both diluted and non-diluted extracts).

3.3. Adapting the method to willowherb samples

3.3.1. Dilution of the extracts

A preliminary qualitative analysis of the samples revealed that the concentration of the oligomeric ETs was inversely proportional to their sizes. The smaller oligomers were very abundant (in all the tissues) whereas the larger ones were scarcer. To ensure that the concentration of all the oligomeric ETs would fall into the linear range, each sample had to be analysed in two different dilutions. The most concentrated one enabled the quantification of pentamer in stems as well as hexamer and heptamer in leaves, flowers and stems. A 32-times diluted version of the extract was thus used to quantify dimer, trimer, tetramer in all the tissues, plus pentamer in leaves and flowers.

3.3.2. Quantification of oenothein B by UV

Another benefit of the 32-times diluted sample was the possibility to quantify oenothein B from the UV trace. The main peak of oenothein B, in the 32-times diluted samples, was analysed by UV and MS and showed a very good purity (Fig. 4). In addition to that, the calibration curve for oenothein B obtained by MRM showed a linear range that spanned only from 0.3 to 15 $\mu g\,mL^{-1}$ ($R^2 = 0.997$) and suffered an almost complete saturation beyond 60 $\mu g\,mL^{-1}$. In comparison, the 280 nm UV calibration curve of oenothein B was linear from 0.3 to 150 $\mu g\,mL^{-1}$ ($R^2 = 0.9984$) which was a more adequate range since diluted leaf and flower samples showed oenothein B concentrations close to 60 $\mu g\,mL^{-1}$. Oenothein B in willowherb should therefore be quantified via UV rather than MS/MS.

3.4. Method validation

3.4.1. Extraction efficiency

In all matrices, tetramer, pentamer, hexamer and heptamer were not detected in the third extract. Dimer and trimer were still present in the third extract but quantification revealed that, in all three matrices, the amount was <1% of the overall extracted quantity. Based on those results it was decided to perform two extraction steps on willowherb samples in order to achieve quantitative extraction (>99%) while minimising sample handling and thus the risk of oxidation of the analytes.

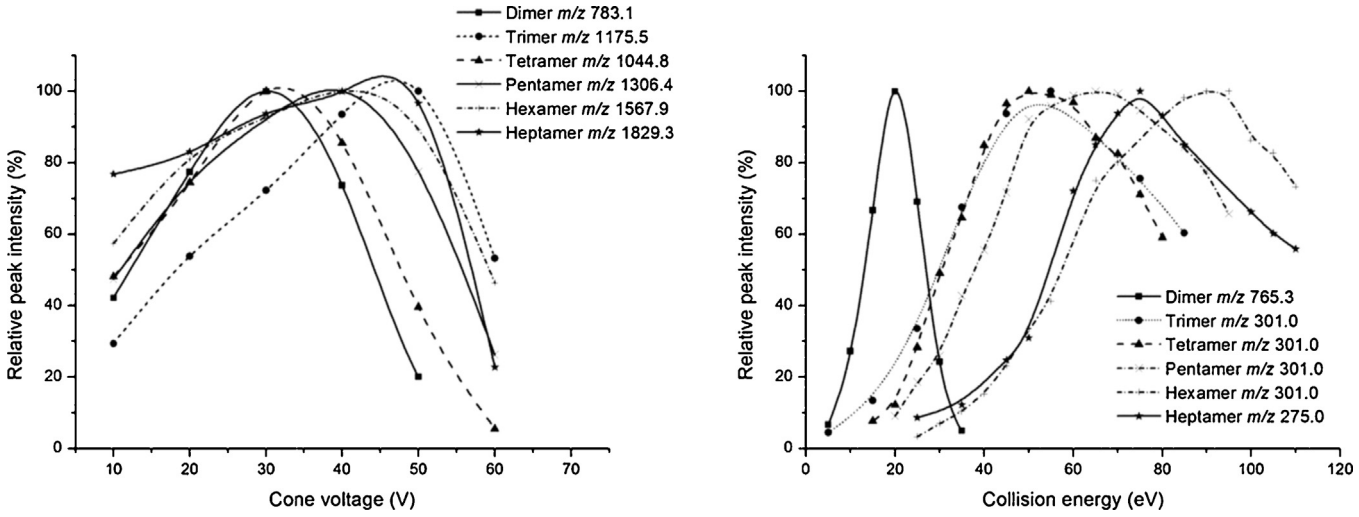

Fig. 3. Optimisation of cone voltage (left-hand side) and collision energy (right-hand side) for the development of MRM transitions. Results are expressed in percentage of the maximum peak intensity measured for each compound and fragment.

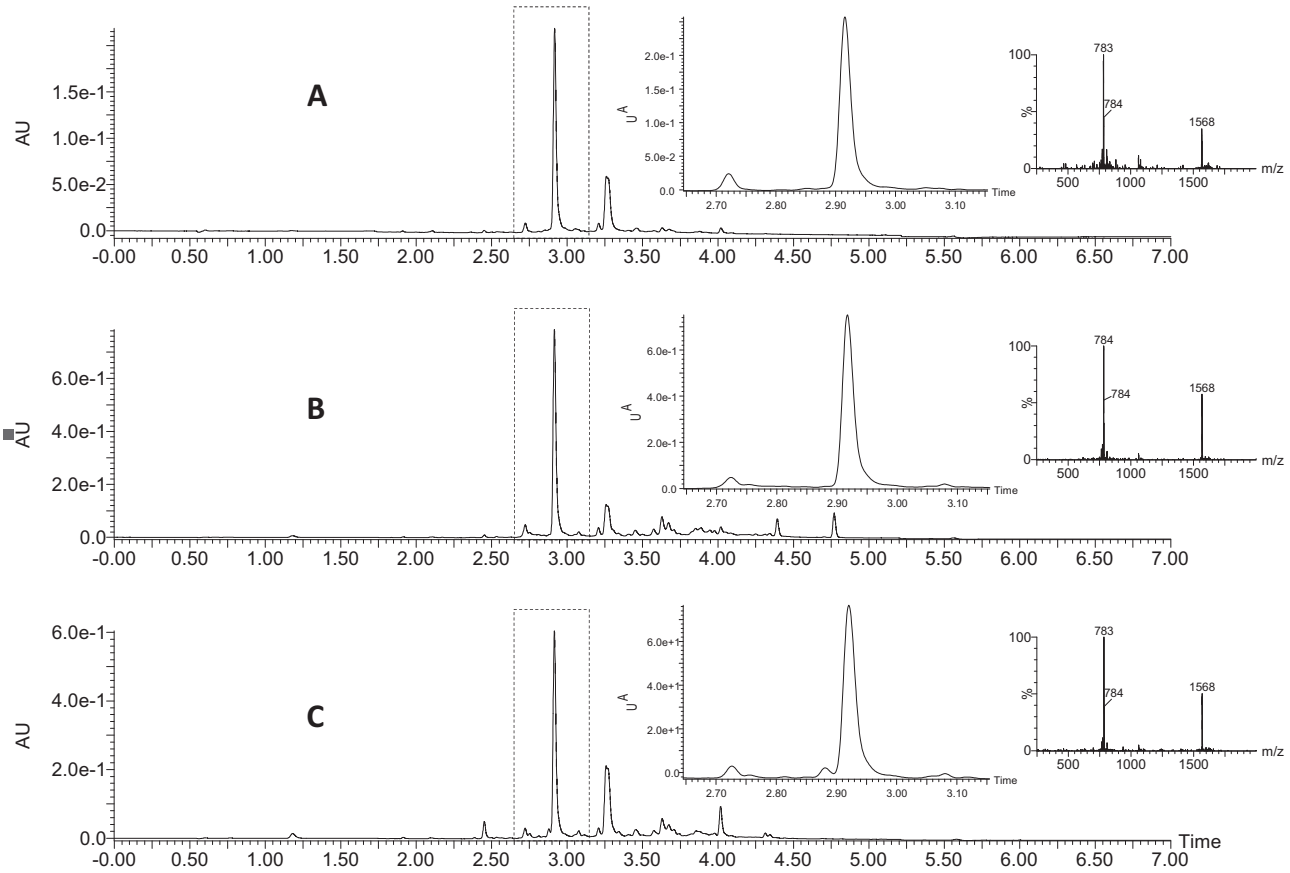

Fig. 4. UV chromatogram (λ = 280 nm) of 32-times diluted extract of *Epilobium angustifolium* stem (A), flower (B) and leaf (C). The inserts show the purity of the main peak in UV and MS.

3.4.2. Calibration curves and linearity

Calibrations curves were fitted with second-order polynomial equations and showed an excellent correlation coefficient ($R^2 > 0.99$). In addition, the linear range was measured for all the plots and the corresponding regression equation and *R*-squared were calculated (Fig. 5). All six compounds showed an excellent linear fit ($R^2 > 0.99$).

3.4.3. Limits of detection and limits of quantification

As shown in Table 3 both LOD and LOQ increase according to the size of the oligomers. Such pattern could be explained by the fact that, the larger the oligomers are, the less efficiently they are ionised in the source, thus resulting in a loss of sensitivity. Regardless of that phenomenon, the LOD and LOQ obtained for each compound with the described method were very low and would allow the quantification of as little as 0.2 mg of heptamer/g of dry plant material. Grancia et al. previously reported a quantification method for oenothein B in *E. angustifolium* by HPLC-DAD and showed a LOQ of 5.62 mg/g of raw material [20]. An HPTLC quantification method for oenothein B in *E. angustifolium* was developed by Shikov et al. [47] and achieved a LOQ of 360 ng/band which corresponded, according to their protocol, to 0.18 mg/g of dry plant material. In the present study the LOQ for oenothein B using UV detection in the diluted extract was 0.88 $\mu g\,mL^{-1}$ which corresponds to 1.41 $mg\,g^{-1}$ and 44 $\mu g\,g^{-1}$ of dry plant material, if quantified from the diluted or non-diluted extracts, respectively. Interestingly, the LOQ for oenothein B using the MRM detection (783.1 > 765.3) was 0.08 $\mu g\,mL^{-1}$, which amounts to 0.13 $mg\,g^{-1}$ or 4 $\mu g\,g^{-1}$of dry plant material, if quantified from the diluted or non-diluted extracts, respectively.

3.4.4. Repeatability

Intra- and inter-assay variability was assessed by measuring the relative standard deviation in the peak area (after correction by the ionisation reference) of dimeric to heptameric ETs in willowherb leaf, flower and stem samples (Table 3). Intra-assay variability ranged from 0.5% to 4.4% and inter-assay variability ranged from 0.9% to 8.1%. Both values generally increased according to the size of the oligomer. However, no clear correlation can be observed regarding a possible influence of the matrix on the stability of the measurements.

3.4.5. Matrix effect

The assessment of the matrix effect showed that for all the analytes quantified by MS/MS from willowherb extracts, the sample matrix caused an underestimation of the true ET concentration. This phenomenon is well known with ESI and has been shown to be largely due to ion suppression caused by co-eluting compounds [48,49]. It can be moderated by sample dilution [50] and that is illustrated in this experiment, where oligomers quantified from diluted samples generally show a much weaker matrix effect than those quantified from non-diluted samples (Table 3). Flower extracts showed to exert the strongest matrix effect on all the oligomers, followed by leaf and stem extracts.

Overall the method proved to be accurate for the quantification of oenothein B, oenothein A and tetrameric TI (in leaf and stem extracts) with matrix effect being <20%. Quantification of pentameric, hexameric and heptameric TI (as well as tetrameric TI in flower extracts), however was significantly affected by the matrix. The accuracy of the quantification of those large oligomers could be improved by finding, for each sample type, the dilution factor that

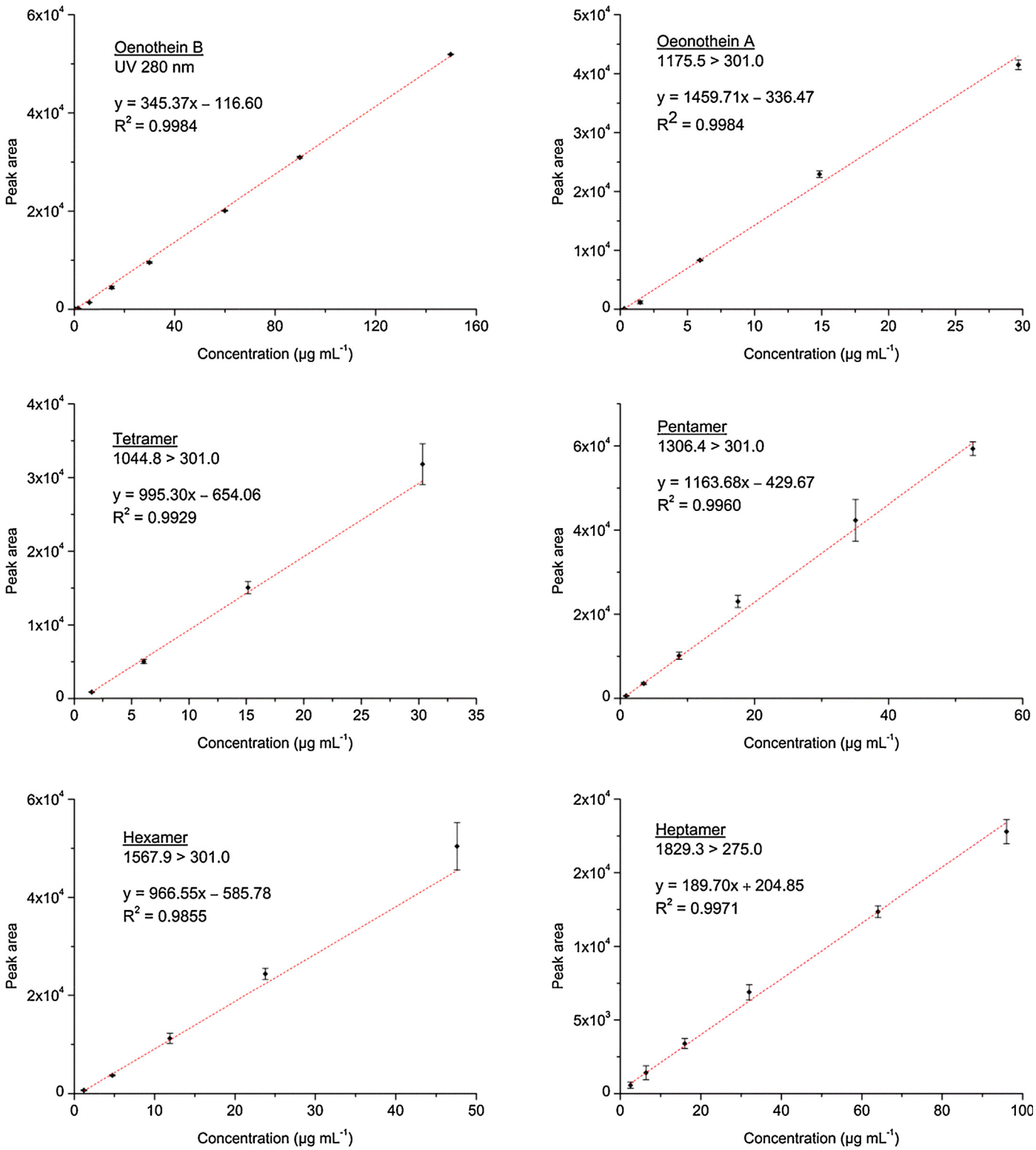

Fig. 5. Calibration curves and linear regression equations of pure dimeric to heptameric ellagitannins. Error bars represent the 95% confidence interval on the estimated mean of the peak area for each data point ($n = 3$).

gives the smallest matrix effect while remaining in the linear range. Alternatively, these complex ETs could be quantified from each sample by the standard addition method. This, however, would require relatively large-scale purification of these rare oligomers and would significantly increase sample preparation and analysis time and per sample.

3.5. Ellagitannins content and distribution in willowherb

To demonstrate the applicability of the method, dimeric to heptameric ETs were quantified from the leaves, flowers and stems of 10 willowherb samples. The results (Fig. 6) first indicate that *E. angustifolium* contains high level of those ETs, which represent

Table 3
Method parameters for the quantification of oligomeric ellagitannins in *Epilobium angustifolium*.

Compound	Quantification method	Sample type for quantification	Linearity ($\mu g\,mL^{-1}$)	LOD ($\mu g\,mL^{-1}$)	LOQ ($\mu g\,mL^{-1}$)	Intra-run RSD (%) $n=30$	Inter-run RSD (%) $n=30$	Matrix effect (%)
Oenothein B	UV 280 nm	32× diluted[a] 32× diluted[b] 32× diluted[c]	0.3–149.8	0.29	0.88	1.1[a] 0.5[b] 0.5[c]	2.2[a] 1.0[b] 0.9[c]	+13.6[a] +15.2[b] +7.4[c]
Oenothein A	MRM 1175.5 > 301.0	32× diluted[a] 32× diluted[b] 32× diluted[c]	0.3–29.7	0.10	0.31	1.1[a] 1.2[b] 1.6[c]	2.5[a] 2.3[b] 4.4[c]	−3.7[a] −1.8[b] −3.7[c]
Tetramer	MRM 1044.8 > 275.0	32× diluted[a] 32× diluted[b] 32× diluted[c]	1.5–30.3	0.34	1.03	2.8[a] 1.1[b] 1.9[c]	4.7[a] 2.2[b] 3.7[c]	−26.8[a] −11.5[b] +2.1[c]
Pentamer	MRM 1306.4 > 301.0	32× diluted[a] 32× diluted[b] Non-diluted[c]	1.2–72.1	0.48	1.44	3.5[a] 2.1[b] 3.8[c]	4.6[a] 3.0[b] 8.1[c]	−70.1[a] −65.4[b] −33.7[c]
Hexamer	MRM 1567.9 > 301.0	Non-diluted[a] Non-diluted[b] Non-diluted[c]	1.2–47.6	0.64	1.92	3.9[a] 3.0[b] NA[c]	6.3[a] 5.9[b] NA[c]	−73.5[a] −64.7[b] NA[c]
Heptamer	MRM 1829.3 > 275.0	Non-diluted[a] Non-diluted[b] Non-diluted[c]	2.6–96.0	1.33	3.98	4.4[a] 3.7[b] NA[c]	4.8[a] 4.7[b] NA[c]	−63.2[a] −39.5[b] NA[c]

[a] Flower samples.
[b] Leaf samples.
[c] Stem samples.

around 15% of the dry mass of flowers and leaves. Oenothein B is the most abundant ET in all three organs and accounts for almost 50% of the total mass of oligomeric ETs. Flowers appeared to contain the highest concentration in all the oligomeric ETs except trimer which was more abundant in leaves. Stems exhibited rather low levels of ETs with hexamer and heptamer being below the limit of quantification.

The inter-individual variations in oligomeric ET content within the sampled population showed interesting patterns. The oligomeric ET content of flowers across the 10 individuals was very stable for the six measured compounds, with RSD ranging from 5.3% (tetramer) to 8.9% (pentamer). However, leaves and stems exhibited larger inter-individual variability. The content in dimeric to tetrameric ET in leaves showed RSD comprised between 7.2 and 8.7%, whereas pentameric to heptameric ETs exhibited RSDs of 13.0% (pentamer) to 21.3% (heptamer). Stems presented even larger variability with RSDs ranging from 10.9% (tetramer) to 30.8% (pentamer).

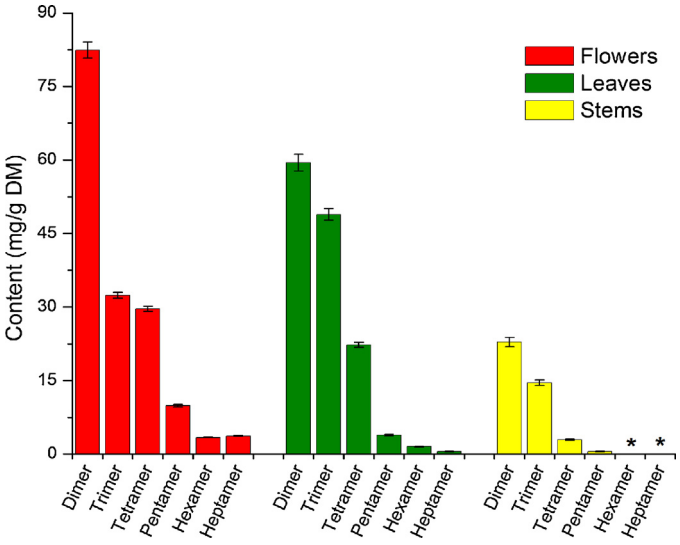

Fig. 6. Organ distribution and content of tellimagrandin I-based oligomeric ellagitannins in willowherb samples ($n=10$). Error bars show standard deviation of the mean. * indicates LOD < quantity < LOQ.

4. Conclusion

This study reports, for the first time, the presence of TI-based oligomeric ETs larger than oenothein A in *E. angustifolium* and describes a method for their isolation and quantification by UHPLC-DAD–ESI-MS/MS. The method proved to be selective, sensitive and stable. It was successfully applied to willowherb samples to assess the quantitative distribution of the oligomeric ETs in the leaves, flowers and stems as well as the inter-individual heterogeneity within a population. The method functioned well with dimers, trimers and tetramers, but suffered from increased matrix effect with pentamers, hexamers and heptamers. However, this shortcoming can be accepted given that there are no isotopically labelled ionisation standards or other quantification methods available for these large tannins that have been very rarely detected in the plant kingdom. This work shows that the development of compound-specific quantification methods is possible, even for exceptionally large hydrolysable tannins, and permits accurate characterisation of the samples.

Funding

These investigations were supported by the European Commission (PITN-GA-2011-289377, "LegumePlus" project) and by the Academy of Finland (Grant no. 258992 to J.-P.S. and 251388 to M.K.).

Acknowledgements

The authors thank Jorma Kim, Tapio Lempiäinen and Atte Tuominen for their invaluable help with sample collection, extraction and preliminary analyses. We address special thanks to Marica Engström for her early contribution to the creation of MRM transitions and for fruitful discussion. We would also like to thank Jari Sinkkonen for his support and comments regarding the redaction of the present article.

Appendix A. Supplementary data

Supplementary data associated with this article can be found, in the online version, at http://dx.doi.org/10.1016/j.chroma.2015.09.050.

References

[1] M.H. Tavendale, L.P. Meagher, D. Pacheco, N. Walker, G.T. Attwood, S. Sivakumaran, Methane production from in vitro rumen incubations with *Lotus pedunculatus* and *Medicago sativa*, and effects of extractable condensed tannin fractions on methanogenesis, Anim. Feed Sci. Technol. 123–124 (2005) 403–419.

[2] A.K. Patra, J. Saxena, A new perspective on the use of plant secondary metabolites to inhibit methanogenesis in the rumen, Phytochemistry 71 (2010) 1198–1222.

[3] D.N. Kamra, N. Agarwal, L.C. Chaudhary, Inhibition of ruminal methanogenesis by tropical plants containing secondary compounds, Int. Congr. Ser. 1293 (2006) 156–163.

[4] A. Novobilský, E. Stringano, C. Hayot Carbonero, L.M.J. Smith, H.L. Enemark, I. Mueller-Harvey, et al., In vitro effects of extracts and purified tannins of sainfoin (*Onobrychis viciifolia*) against two cattle nematodes, Vet. Parasitol. 196 (2013) 532–537.

[5] H. Hoste, F. Jackson, S. Athanasiadou, S.M. Thamsborg, S.O. Hoskin, The effects of tannin-rich plants on parasitic nematodes in ruminants, Trends Parasitol. 22 (2006) 253–261.

[6] J.-P. Salminen, T. Roslin, M. Karonen, J. Sinkkonen, K. Pihlaja, P. Pulkkinen, Seasonal variation in the content of hydrolyzable tannins, flavonoid glycosides, and proanthocyanidins in oak leaves, J. Chem. Ecol. 30 (2004) 1693–1711.

[7] J.-P. Salminen, V. Ossipov, E. Haukioja, K. Pihlaja, Seasonal variation in the content of hydrolysable tannins in leaves of *Betula pubescens*, Phytochemistry 57 (2001) 15–22.

[8] C.T. Yarnes, W.J. Boecklen, J.-P. Salminen, No simple sum: seasonal variation in tannin phenotypes and leaf-miners in hybrid oaks, Chemoecology 18 (2007) 39–51.

[9] J.-P. Salminen, V. Ossipov, K. Pihlaja, Distribution of hydrolysable tannins in the foliage of Finnish birch species, Z. Naturforsch. C 57 (2002) 248–256.

[10] A. Tuominen, E. Toivonen, P. Mutikainen, J.-P. Salminen, Defensive strategies in *Geranium sylvaticum*. Part 1: Organ-specific distribution of water-soluble tannins, flavonoids and phenolic acids, Phytochemistry 95 (2013) 394–407.

[11] H. Kawamoto, F. Nakatsubo, Solubility of protein complexed with galloylglucoses, Phytochemistry 30 (1997) 485–488.

[12] H.-C. Zhou, Y.-M. Lin, S.-D. Wei, N.F. Tam, Structural diversity and antioxidant activity of condensed tannins fractionated from mangosteen pericarp, Food Chem. 129 (2011) 1710–1720.

[13] M. Labieniec, T. Gabryelak, G. Falcioni, Antioxidant and pro-oxidant effects of tannins in digestive cells of the freshwater mussel *Unio tumidus*, Mutat. Res. Toxicol. Environ. Mutagen. 539 (2003) 19–28.

[14] E. Bouki, V.K. Dimitriadis, M. Kaloyianni, S. Dailianis, Antioxidant and pro-oxidant challenge of tannic acid in mussel hemocytes exposed to cadmium, Mar. Environ. Res. 85 (2013) 13–20.

[15] S.M. Hadi, S.H. Bhat, A.S. Azmi, S. Hanif, U. Shamim, M.F. Ullah, Oxidative breakage of cellular DNA by plant polyphenols: a putative mechanism for anticancer properties, Semin. Cancer Biol. 17 (2007) 370–376.

[16] P. Arapitsas, Hydrolyzable tannin analysis in food, Food Chem. 135 (2012) 1708–1717.

[17] P. Schofield, D.M. Mbugua, A.N. Pell, Analysis of condensed tannins: a review, Anim. Feed Sci. Technol. 91 (2001) 21–40.

[18] J.L. Aleixandre-Tudo, H. Nieuwoudt, J.L. Aleixandre, W.J. Du Toit, Robust ultraviolet–visible (UV–vis) partial least-squares (PLS) models for tannin quantification in red wine, J. Agric. Food Chem. 63 (2015) 1088–1098.

[19] K. Komatsu, Y. Nagayama, K. Tanaka, Y. Ling, P. Basnet, M.R. Meselhy, Development of a high performance liquid chromatographic method for systematic quantitative analysis of chemical constituents in rhubarb, Chem. Pharm. Bull. (Tokyo) 54 (2006) 941–947.

[20] S. Granica, A. Bazylko, A.K. Kiss, Determination of macrocyclic ellagitannin oenothein B in plant materials by HPLC-DAD–MS: method development and validation, Phytochem. Anal. 23 (2012) 582–587.

[21] D. Guillarme, J. Schappler, S. Rudaz, J.-L. Veuthey, Coupling ultra-high-pressure liquid chromatography with mass spectrometry, Trends Anal. Chem. 29 (2010) 15–27.

[22] M. Rodriguez-Aller, R. Gurny, J.-L. Veuthey, D. Guillarme, Coupling ultra high-pressure liquid chromatography with mass spectrometry: constraints and possible applications, J. Chromatogr. A 1292 (2012) 2–18.

[23] C. Lo, J.C.Y. Le Blanc, C.K.Y. Yu, K.H. Sze, D.C.M. Ng, I.K. Chu, Detection, characterization, and quantification of resveratrol glycosides in transgenic arabidopsis over-expressing a sorghum stilbene synthase gene by liquid chromatography/tandem mass spectrometry, Rapid Commun. Mass Spectrom. 21 (2007) 4101–4108.

[24] S. Forcat, M.H. Bennett, J.W. Mansfield, M.R. Grant, A rapid and robust method for simultaneously measuring changes in the phytohormones ABA, JA and SA in plants following biotic and abiotic stress, Plant Methods 4 (2008) 16.

[25] E. Ruszová, J. Cheel, S. Pávek, M. Moravcová, M. Hermannová, I. Matějková, et al., *Epilobium angustifolium* extract demonstrates multiple effects on dermal fibroblasts in vitro and skin photo-protection in vivo, Gen. Physiol. Biophys. 32 (2013) 347–359.

[26] A.K. Kiss, J. Kowalski, M.F. Melzig, Effect of *Epilobium angustifolium* L. extracts and polyphenols on cell proliferation and neutral endopeptidase activity in selected cell lines, Pharmazie 61 (2006) 66–69.

[27] I. Kosalec, N. Kopjar, D. Kremer, Antimicrobial activity of willowherb (*Epilobium angustifolium* L.) leaves and flowers, Curr. Drug Targets 14 (2013) 986–991.

[28] S. Granica, J.P. Piwowarski, M.E. Czerwińska, A.K. Kiss, Phytochemistry, pharmacology and traditional uses of different Epilobium species (Onagraceae): a review, J. Ethnopharmacol. 156 (2014) 316–346.

[29] A.K. Kiss, A. Bazylko, A. Filipek, S. Granica, E. Jaszewska, U. Kiarszys, et al., Oenothein B's contribution to the anti-inflammatory and antioxidant activity of *Epilobium* sp, Phytomedicine 18 (2011) 557–560.

[30] A.G. Ramstead, I.A. Schepetkin, M.T. Quinn, M.A. Jutila, Oenothein B, a cyclic dimeric ellagitannin isolated from *Epilobium angustifolium*, enhances IFNγ production by lymphocytes, PLoS ONE 7 (2012).

[31] T. Yoshida, T. Hatano, H. Ito, Chemistry and function of vegetable polyphenols with high molecular weights, Biofactors 13 (2000) 121–125.

[32] H. Li, T. Tanaka, Y.-J. Zhang, C.-R. Yang, I. Kouno, Rubusuaviins A-F, monomeric and oligomeric ellagitannins from Chinese sweet tea and their alpha-amylase inhibitory activity, Chem. Pharm. Bull. (Tokyo) 55 (2007) 1325–1331.

[33] Y.J. Tsai, T. Aoki, H. Maruta, H. Abe, H. Sakagami, T. Hatano, et al., Mouse mammary tumor virus gene expression is suppressed by oligomeric ellagitannins, novel inhibitors of poly(ADP-ribose) glycohydrolase, J. Biol. Chem. 267 (1992) 14436–14442.

[34] H. Ito, P. Li, M. Koreishi, A. Nagatomo, N. Nishida, T. Yoshida, Ellagitannin oligomers and a neolignan from pomegranate arils and their inhibitory effects on the formation of advanced glycation end products, Food Chem. 152 (2014) 323–330.

[35] Elias Lönnrotin Flora Fennica III, in: K. Linnilä, S. Savikko, T. Lempiäinen (Eds.), Elias Lönnrotin Flora Fenn III, Oy Amanita Ltd, Hämeenlinna, 2002, p. 148.

[36] L.M. Katiki, J.F.S. Ferreira, J.M. Gonzalez, A.M. Zajac, D.S. Lindsay, A.C.S. Chagas, et al., Anthelmintic effect of plant extracts containing condensed and hydrolyzable tannins on *Caenorhabditis elegans*, and their antioxidant capacity, Vet. Parasitol. 192 (2013) 218–227.

[37] R. Bhatta, Y. Uyeno, K. Tajima, A. Takenaka, Y. Yabumoto, I. Nonaka, et al., Difference in the nature of tannins on in vitro ruminal methane and volatile fatty acid production and on methanogenic archaea and protozoal populations, J. Dairy Sci. 92 (2009) 5512–5522.

[38] W.F. Pellikaan, E. Stringano, J. Leenaars, D.J.G.M. Bongers, S. van Schuppen-van Laar, J. Plant, et al., Evaluating effects of tannins on extent and rate of in vitro gas and CH4 production using an automated pressure evaluation system (APES), Anim. Feed Sci. Technol. 166–167 (2011) 377–390.

[39] D.R. Mani, S.E. Abbatiello, S.A. Carr, Statistical characterization of multiple-reaction monitoring mass spectrometry (MRM-MS) assays for quantitative proteomics, BMC Bioinformatics 13 (Suppl. 1) (2012) S9.

[40] M. Caban, N. Migowska, P. Stepnowski, M. Kwiatkowski, J. Kumirska, Matrix effects and recovery calculations in analyses of pharmaceuticals based on the determination of β-blockers and β-agonists in environmental samples, J. Chromatogr. A 1258 (2012) 117–127.

[41] B. Ducrey, A. Marston, S. Göhring, R.W. Hartmann, K. Hostettmann, Inhibition of 5 alpha-reductase and aromatase by the ellagitannins oenothein A and oenothein B from Epilobium species, Planta Med. 63 (1997) 111–114.

[42] T. Yoshida, T. Hatano, T. Okuda, Two-dimensional NMR spectra of hydrolysable tannins which form equilibrium mixtures, Magn. Reson. Chem. 30 (1992) 46–55.

[43] T. Yoshida, T. Chou, M. Matsuda, T. Yasuhara, K. Yazaki, T. Hatano, et al., Woodfordin D and oenothein A, trimeric hydrolyzable tannins of macrocyclic structure with antitumor activity, Chem. Pharm. Bull. (Tokyo) 39 (1991) 1157–1162.

[44] M. Karonen, J. Parker, A.A. Agrawal, J.-P. Salminen, First evidence of hexameric and heptameric ellagitannins in plants detected by liquid chromatography/electrospray ionisation mass spectrometry, Rapid Commun. Mass Spectrom. 24 (2010) 3151–3156.

[45] J.-P. Salminen, M. Karonen, J. Sinkkonen, Chemical ecology of tannins: recent developments in tannin chemistry reveal new structures and structure–activity patterns, Chem. Eur. J. 17 (2011) 2806–2816.

[46] T. Hooi Poay, L. Sui Kiong, C. Cheng Hock, Characterisation of galloylated cyanogenic glucosides and hydrolysable tannins from leaves of *Phyllagathis rotundifolia* by LC–ESI-MS/MS, Phytochem. Anal. 22 (2011) 516–525.

[47] A.N. Shikov, O.N. Pozharitskaya, S.A. Ivanova, V.G. Makarov, V.P. Tikhonov, B. Galambosi, Improved and validated HPTLC method for quantification of oenothein B and its use for analysis of *Epilobium angustifolium* L, J. Planar Chromatogr. 23 (2010) 70–74.

[48] R. King, R. Bonfiglio, C. Fernandez-Metzler, C. Miller-Stein, T. Olah, Mechanistic investigation of ionization suppression in electrospray ionization, J. Am. Soc. Mass Spectrom. 11 (2000) 942–950.

[49] P. Kebarle, L. Tang, From ions in solution to ions in the gas phase – the mechanism of electrospray mass spectrometry, Anal. Chem. 65 (1993) 972A–986A.

[50] A. Kruve, I. Leito, K. Herodes, Combating matrix effects in LC/ESI/MS: the extrapolative dilution approach, Anal. Chim. Acta 651 (2009) 75–80.